

Intermediate mass fragments from the reactions 486, 550, 640, and 730 MeV $^{86}\text{Kr} + ^{63}\text{Cu}$

J. Boger,* John M. Alexander, A. Elmaani,[†] S. Kox,[‡] Roy A. Lacey, and A. Narayanan[§]
Department of Chemistry, State University of New York at Stony Brook, Stony Brook, New York 11794

D. J. Moses
Department of Chemistry, Carnegie Mellon University, Pittsburgh, Pennsylvania 15213

M. A. McMahan
Lawrence Berkeley Laboratory, Berkeley, California 94720

P. A. DeYoung and C. J. Gelderloos^{||}
Department of Physics, Hope College, Holland, Michigan 49423
(Received 28 April 1993)

Intermediate mass fragments have been studied from the reaction $^{86}\text{Kr} + ^{63}\text{Cu}$ for ^{86}Kr beam energies of 486, 550, 640, and 730 MeV. Average center-of-mass (c.m.) energies are nearly constant with the c.m. angle and vary little with incident energy. Furthermore, the angular distributions are well approximated by $1/\sin\theta_{\text{c.m.}}$. From this and other evidence we conclude that equilibration has occurred prior to fissionlike asymmetric binary breakup of the composite nucleus in the predominant mechanism for IMF production.

PACS number(s): 24.60.Dr, 25.70.Gh, 25.70.Jj

I. INTRODUCTION

In recent years, unfolding the mechanisms and sources of intermediate mass fragment (IMF) production has been a major goal of heavy-ion reaction studies (see, for example, Ref. [1] and references therein). The attempt to distinguish simultaneous multifragmentation from sequential binary fission, for example, has become a major challenge (e.g., [2,3]). Much of this work, however, has been done with incident energies $\geq 20A$ MeV. For these relatively high incident velocities, it is particularly difficult to identify the mechanisms responsible for IMF production because incomplete fusion and deeply inelastic reactions lead to a broad range of energy depositions. For lower energies (E/A of $\lesssim 10$ MeV) the situation is quite different. The more central collisions lead to essentially complete fusion so that one can easily characterize the total excitation energy of the equilibrated composite systems. For the IMF's, we must ask if they are indeed ejected from such equilibrated composite nuclei. If so,

then we can use their emission probabilities, energies, etc., to probe their formation barriers and other properties of the emitting systems.

In this paper we report experimental results for inclusive IMF measurements from four reactions: 486, 550, 640, and 730 MeV $^{86}\text{Kr} + ^{63}\text{Cu}$. Initial excitation energies for complete fusion range from 125 to 231 MeV, and cross sections for IMF's increase rapidly (e.g., for ^{12}C from 0.9 to 14 mb). Observations of the IMF energy spectra, angular distributions, yields, and dimensionless cross sections lead to the conclusion that, for these reactions, there is indeed equilibration after the fusion of target and projectile. A subsequent asymmetric binary fission like breakup is the major source of IMF emission [4]. In a forthcoming paper [5], we analyze the IMF excitation functions within the framework of the statistical model in an attempt to extract IMF fission barriers.

II. EXPERIMENTAL SETUP

The Berkeley SuperHILAC provided beams of 486, 550, 640, and 730 MeV ^{86}Kr , which bombarded a ^{63}Cu target of thickness $1030 \mu\text{g}/\text{cm}^2$. Two "wedge" detectors [6], for registration of ^4He and heavier particles, were placed symmetrically on either side of the beam. These detectors are composed of 5 coplanar solid-state stopping detectors (≈ 4.5 msr) spaced radially every 10° and have a common gas ionization chamber to provide the ΔE signal. Angular positions for the stopping detectors in each wedge were from 38° to 78° . Additionally, three individual gas ionization chambers (equipped with solid-state stopping detectors) were placed, one each, at 18° above

*Present address: Texas A&M University, Cyclotron Institute, College Station, TX 77843-3366.

[†]Present address: University of Washington, Nuclear Physics Lab GL-10, Seattle, WA 98195.

[‡]Present address: Institut des Sciences Nucléaires, 53 ave. des Martyrs, 38026 Grenoble, Cedex, France.

[§]Present address: Dept. of Chemistry, Brock University, St. Catharines, Ontario, Canada L2S 3A1.

^{||}Present address: Department of Physics, State University of New York at Stony Brook, Stony Brook, NY 11794.

and below the beam and one at -18° to the beam in the same plane as the wedge detectors. Kinematic and detector thresholds for the IMF's were such that three angles were most important for measuring the c.m. energy spectra. These were the lab angles of 18° , 38° , and 48° . For the 550 and 640 MeV reactions, the detectors were also moved to other angles for short counting periods.

Identification of the IMF's by charge (Z) was made from ΔE - E scatterplots. Individual Z identification for $Z \leq 24$ was achieved for the 550 and 640 MeV reactions, and for $Z \leq 22$ for the 486 and 730 MeV reactions. The relative intensity of ^4He was so great that the neighboring Li fragments could not be completely separated. Laboratory energy spectra were corrected for energy losses in the target and in the detector cover foils. These spectra were then converted event-by-event into the center of mass. Average beam currents were typically ≈ 5 nA. More details are given in Ref. [7].

III. RESULTS AND DISCUSSION

Figures 1–4 present c.m. kinetic energy spectra for IMF's of $5 \leq Z \leq 14$ for the 640 and 730 MeV ^{86}Kr reactions. They have also been measured for the 486 and 550 MeV reactions. These IMF energy spectra do not include the recoil of the complementary fragments and thus do not give total kinetic energies. These energies refer to the primary fragments, the masses of which have been estimated from IMF-particle coincidence multiplicities as described in Ref. [8]. Note the near Gaussian shapes of the high energy peaks shown in Figs. 1–4. For a given Z , the average c.m. energies are constant (or nearly so) with angle. In Figs. 5 and 6, we show the average kinetic energies and their standard deviations as a function of the initial excitation energy of the fused composite nucleus. Figures 5 and 6 (left) show that average c.m. energies are essentially constant over the excitation energy range studied here. However, the standard deviations (right) increase with increasing excitation energy.

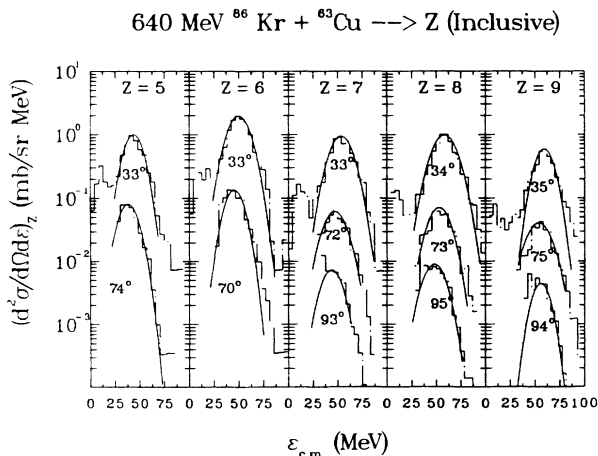


FIG. 1. Inclusive c.m. energy spectra for primary intermediate mass fragments $5 \leq Z \leq 9$ at indicated c.m. angles for the reaction $640 \text{ MeV } ^{86}\text{Kr} + ^{63}\text{Cu}$.

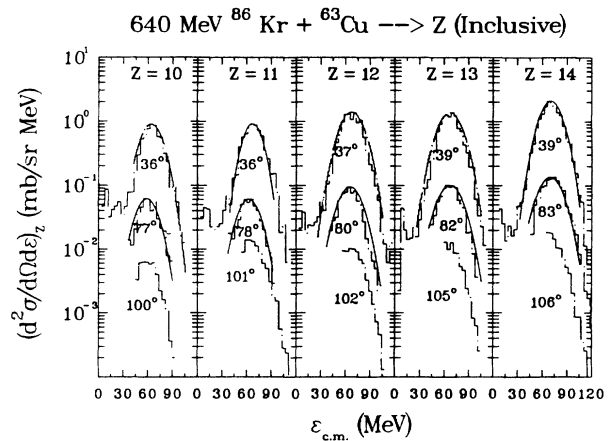


FIG. 2. Same as Fig. 1, but for $10 \leq Z \leq 14$.

The fact that the energies are constant with bombarding energy is particularly revealing. It supports the conclusion that the emission of an IMF follows the equilibration of a composite nucleus. If a fast process such as projectile breakup were involved in their production, then we would expect some remnant of the velocity of the projectile to be retained throughout the reaction process. We would therefore expect the energy of an IMF to increase with an increase in bombarding energy. Since this is not observed, fusion of projectile and target seems to be the preferred reaction path. Fast reaction processes for IMF production are not ruled out in general. They simply appear not to be a major reaction mechanism for the energies and angular regions of this study. This observation and conclusion is consistent with those from the ‘‘Coulomb rings’’ observed in similar reactions [9,10]. These ‘‘rings’’ give a qualitative overall test for isotropic emission from a single moving source.

The Gaussian spectral shapes over this excitation energy range also indicate that the emission is not strongly driven by the temperature of the emitter [11]. By con-

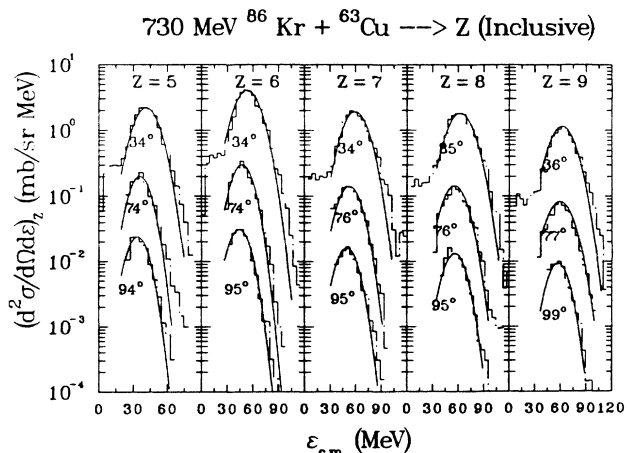


FIG. 3. Same as Fig. 1, but for the reaction $730 \text{ MeV } ^{86}\text{Kr} + ^{63}\text{Cu}$.

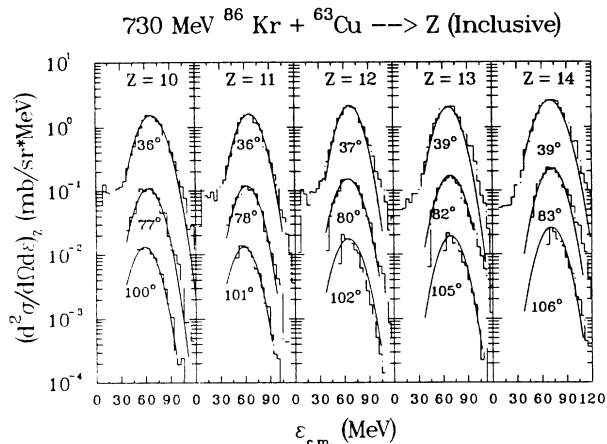


FIG. 4. Same as Fig. 2, but for the reaction 730 MeV $^{86}\text{Kr} + ^{63}\text{Cu}$.

trast, we observe quite different energy spectra for ^4He , as shown in Fig. 7. These Maxwellian-like energy spectra, shown for three energies, have high-energy slopes that decrease (or become harder) with an increase in temperature of the emitter. For the IMF's, the Coulomb repulsion between the fragments seems to dominate and to lead to Gaussian shapes in this energy regime. By contrast, IMF energy spectra with such Maxwellian shapes have already been observed in the reaction of $^{40}\text{Ar} + ^{\text{nat}}\text{Ag}$ at 17 MeV per nucleon [12], indicating that the emitter temperature does play an increasingly important role for higher incident energies (see Ref. [13] as well).

Note that the right-hand sides of Figs. 5 and 6 show that the width of these spectra broaden with increas-

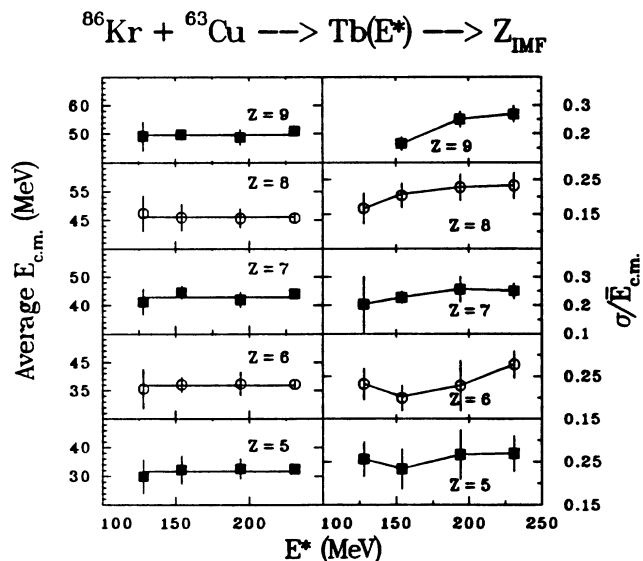


FIG. 5. Left-hand side: Average c.m. kinetic energies for $\theta_{\text{c.m.}} \approx 75^\circ$ for IMF's of $5 \leq Z \leq 9$ versus excitation energy, E^* . The straight line is the kinetic energy averaged over the excitation energy. Right-hand side: Standard deviation of the energy spectra divided by the average energy.

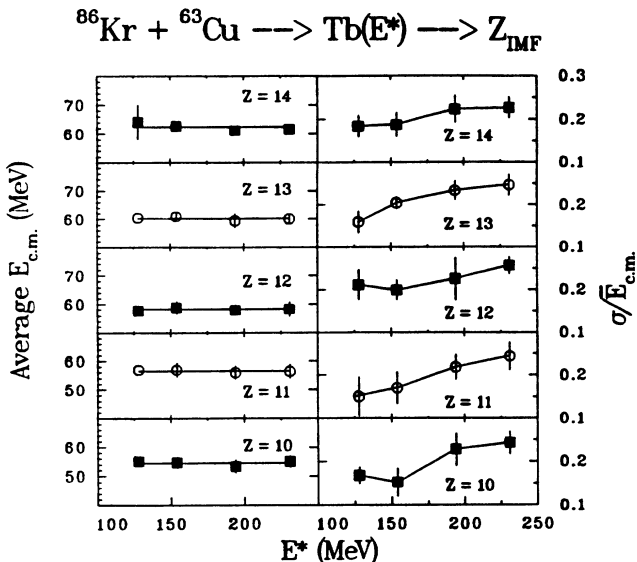


FIG. 6. Same as Fig. 5, but for IMF's of Z's 10-14.

ing excitation energy. These figures plot the fractional width $\sigma / \langle E_{\text{c.m.}} \rangle$ as a function of excitation energy, where σ is the standard deviation derived from the Gaussian fits shown in Figs. 1-4. As the value of $\langle E_{\text{c.m.}} \rangle$ shows little dependence on excitation energy, the increase in $\sigma / \langle E_{\text{c.m.}} \rangle$ simply reflects the growth in σ with excitation energy. This growth could possibly be attributed to

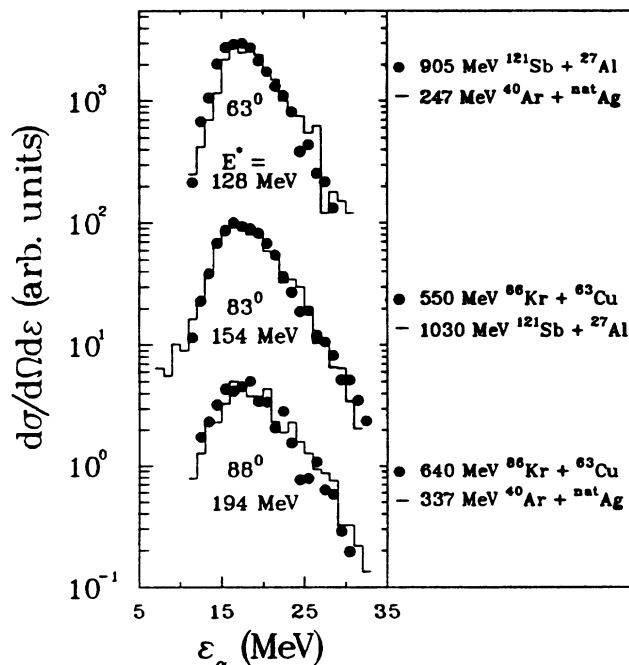


FIG. 7. Energy spectra for ^4He in coincidence with ^4He for three excitation energies: 128, 154, and 194 MeV. Reactions are indicated. Energy spectrum from the $^{121}\text{Sb} + ^{27}\text{Al}$ reaction is taken from Ref. [17].

the excitation of additional collective modes: vibrational, torsional, bending, and stretching. These may be functions of the excitation energy [14] and may broaden the energy spectra as one marches up in excitation energy.

Note that the c.m. energy spectra (Figs. 1–4) are nearly invariant with angle. This also suggests a long-lived intermediate, one that has a lifetime comparable to its rotational period, signifying a loss of memory of entrance channel direction. This places the production of the IMF's in a reaction class that is longer than the time needed for complete fusion. If they were produced in fast reactions, then the energies would drop off rapidly with respect to the beam direction, as projectile like fragments retain their sense of direction and velocity throughout the reaction.

Angular distributions for IMF's of $4 \leq Z \leq 14$ are shown in Figs. 8 and 9 for the 640 and 730 MeV reactions. As these IMF's were produced in reactions employing reversed kinematics, the forward peaking in the angular distributions shown in Figs. 8 and 9 is actually backward peaking with respect to the light reaction partner [15]. Also shown as dashed lines are $1/\sin\theta_{c.m.}$ fits to the data; this is the expected behavior for a fission reaction. Overall, these fits reproduce the angular distributions rather well and also support the conclusion that the predominant mode of IMF formation is essentially asymmetric binary fission following compound nucleus formation. Coincidence measurements from Ref. [4] also indicate only a very small presence of ternary breakup processes.

These angular distributions have been integrated by using the $1/\sin\theta_{c.m.}$ fits, and the resulting cross sections

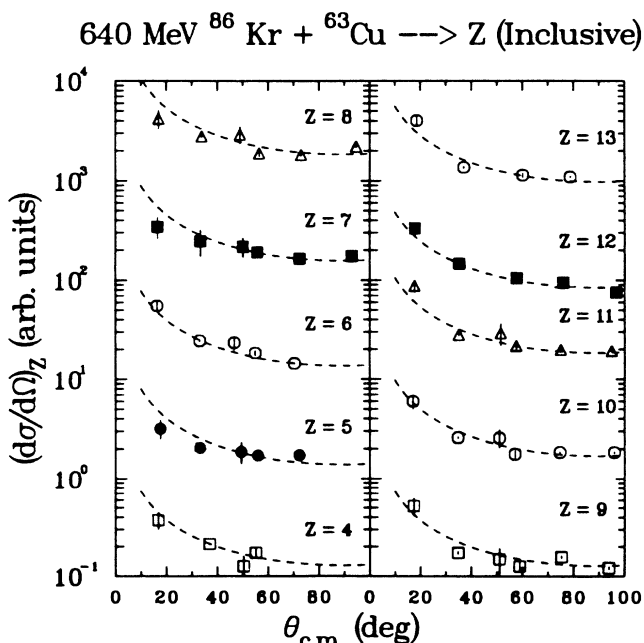


FIG. 8. Angular distributions for IMF's of $4 \leq Z \leq 13$ for the 640 MeV reaction. Dashed lines are $1/\sin\theta_{c.m.}$ distributions that have been normalized to the data. Error bars are statistical.

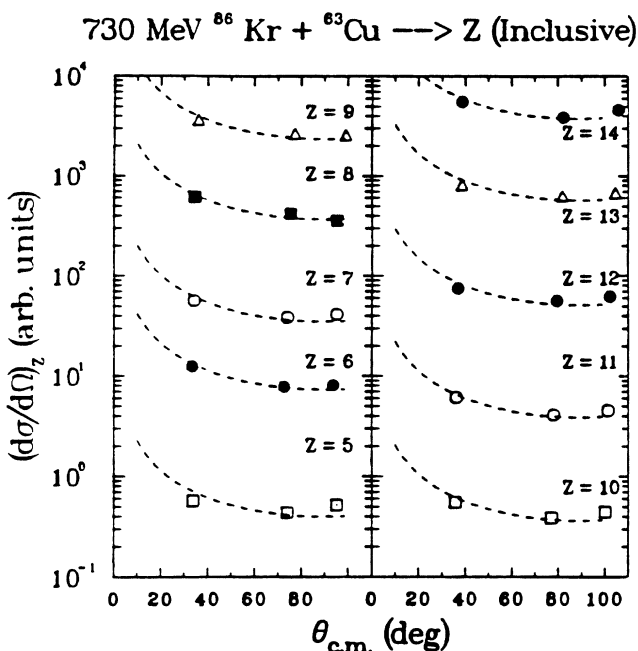


FIG. 9. Same as Fig. 8, but for the 730 MeV reaction and for IMF's of Z 's 5–14.

are shown in Fig. 10 along with those for ^1H and ^4He . For all excitation energies, the largest cross sections are for $Z = 1$ and 2; they are much smaller for $Z \approx 3$ –10 with a gradual increase from $Z \approx 10$ to 24. This trend is most dramatic for 486 MeV. The steepness of the slope for $Z \geq 10$ decreases as one increases in excitation energy. The production of the IMF's, which is strongly disfavored at low energy, becomes increasingly favored with increasing

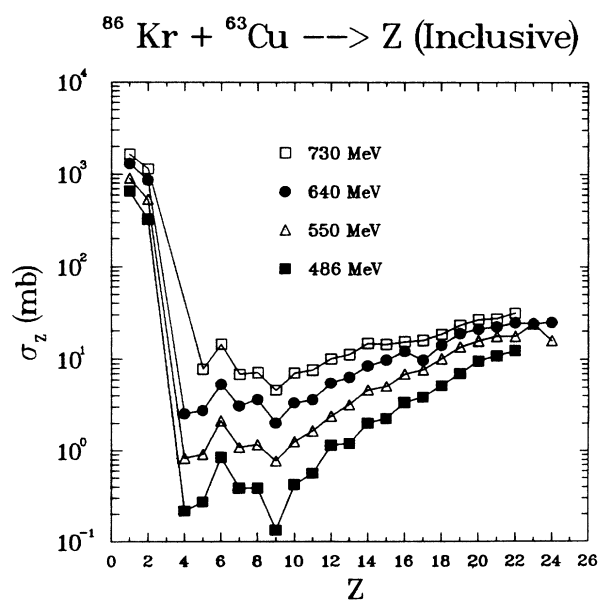


FIG. 10. Inclusive angle-integrated cross sections for the four ^{86}Kr incident energies shown.

excitation energy.

Also note in Fig. 10 the enhanced cross sections for $Z=6$, and the depressed cross sections for $Z=9$. This effect, most notable for the 486 MeV reaction, is often identified as a “shell effect” (see, e.g., [16]), which may arise at scission or in the post scission evaporation. As the primary IMF’s are born with some excitation energy, they may undergo further decay through the evaporation of light particles. Binding energies are often larger for light IMF’s of even Z than for those of odd Z . Primary IMF’s with odd charge thus have a greater probability for further decay. This enhancement in the carbon cross section may then result partially from its preferential formation by evaporation from such primary decay products. However, it is true that the experimentally derived postscission particle multiplicities are small [8]; hence it is likely that the shell effects arise mainly from the primary formation probabilities.

We now compare dimensionless IMF cross sections produced in two entrance channels. A dimensionless IMF cross section, $\sigma_{\text{IMF}}(E^*)/\pi(\lambda/2\pi)^2$, is defined as follows:

$$\frac{\sigma_{\text{IMF}}}{\pi\lambda^2}(E^*) = \sum_{\ell_{\text{min}}}^{\ell_{\text{max}}} (2\ell + 1) P(\ell, E^*) \quad (3.1)$$

with excitation energy E^* , entrance channel wavelength (λ), and orbital angular momentum ℓ . The exit channel factor $P(\ell, E^*)$ represents the spin and excitation-energy dependent decay probabilities for the emission of an IMF. We note that division of the experimental cross section by the entrance-channel dependent term $\pi\lambda^2$ leaves a summation over only exit-channel spin-dependent decay probabilities. If these decay probabilities are indeed decided by the composite nucleus, then dimensionless cross sections should agree for matched entrance channels (i.e., matched in E^* and covering the relevant spin zone).

Reference [17] reported IMF cross sections up to $Z=9$ from the reaction 337 MeV $^{40}\text{Ar} + \text{nat}\text{Ag}$. This system matches in excitation energy the 640 MeV ^{86}Kr reaction ($E^*=194$ MeV). Dimensionless cross sections are compared in Table I for these two systems. The general agreement between these two entrance channels provides additional evidence that the IMF’s in this energy regime are produced by compound-nucleus reactions. The discrepancy for Li may be due to the overwhelming presence of ^4He , which was great enough to make it difficult to achieve complete separation.

It has been very common in heavy-ion reaction studies to classify reaction groups by their major heavy fragments, i.e., evaporation residues (ER’s), fusion fission (FF), deeply inelastic reactions (DIR), and quasielastic reactions (QER). These classifications have also served as guides to the spin zones involved.

At low energies (e.g., 486 MeV in Fig. 10) there is a deep valley in σ_z for $3 \lesssim Z \lesssim 12$, which serves to separate the FF group from the ER group produced after the particle evaporation (e.g., n , H and He “particles”). An IMF emission of $3 \lesssim Z \lesssim 12$ actually leaves behind a heavy nuclear residue that is included in the ER group.

TABLE I. IMF dimensionless cross sections.

Particle	Dimensionless cross sections, $\sigma_{\text{IMF}}/\pi\lambda^2$	
	337 MeV $^{40}\text{Ar} + \text{nat}\text{Ag}$	640 MeV $^{86}\text{Kr} + ^{63}\text{Cu}$
^1H	20360 \pm 610	17020 \pm 630
^2H	1820 \pm 180	1770 \pm 200
^3H	612 \pm 61	740 \pm 120
^4He	13300 \pm 400	13500 \pm 1350
Li	94 \pm 14	187 \pm 4
Be	47 \pm 7	38 \pm 1.2
B	37 \pm 6	41 \pm 1.3
C	81 \pm 12	80 \pm 1.9
N	79 \pm 12	46 \pm 2.1
O	43 \pm 6	54 \pm 2.4
F	49 \pm 7	30 \pm 1.6

As the yield of these IMF’s increase with incident energy, their production generates such heavy nuclei in the ER class, but with broader angular distributions than calculated for evaporation of only n , H and He particles [18]. At higher energies, or in any situation where there is no distinct valley in σ_z , there will be no clear separation between the ER and FF groups. For the reactions and energies studied here the IMF’s of $Z \lesssim 12$ to 20 will be included in the ER group, which retains a rather clear distinction from the FF group. The fragments of $Z \gtrsim 12$ will generally be classified as a part of the FF group. However, such distinctions may not be completely clear and may be decided essentially by the taste of the experimenters.

In conclusion, a coherent picture emerges that the dominant pathway for the production of these IMF’s is a binary fissionlike breakup following fusion of target and projectile. This view is supported by several observations: (1) the average IMF energies are essentially constant with varying bombarding energy; (2) for a given bombarding energy, the mean energies are nearly invariant with c.m. angle; (3) dimensionless cross sections for inclusive IMF’s show broad agreement for matched entrance channels; and (4) backward peaking of the angular distributions with respect to the light reaction partner follows $1/\sin\theta_{\text{c.m.}}$, the classical limit for the binary emission of a fragment from a rapidly rotating system. Coincidence measurements in Ref. [4] also indicate only a very small presence of ternary breakup processes.

ACKNOWLEDGMENTS

The staff of the Lawrence Berkeley Laboratory Super-Hilac is gratefully acknowledged. This work was supported by the Division of Nuclear Physics, Office of High Energy and Nuclear Physics, U.S. Department of Energy. We thank E. Vardaci and M. Kaplan for discussions and useful exchanges concerning calibrations, analysis techniques, etc.

- [1] V. E. Viola, J. L. Wile, D. E. Fields, K. Kwiatkowski, S. J. Yennello, H. M. Xu, M. B. Tsang, R. T. deSouza, E. Renshaw, J. Pochodzalla, K. B. Morley, W. G. Lynch, W. G. Gong, C. K. Gelbke, D. J. Fields, and N. Carlin, *Nucl. Phys.* **A538**, 291c (1992).
- [2] K. Hagel, M. Gonin, R. Wada, J. B. Natowitz, B. H. Sa, Y. Lou, M. Gui, D. Utley, G. Nebbia, D. Fabris, G. Prete, J. Ruiz, D. Drain, B. Chambon, B. Cheynis, D. Guinet, X. C. Hu, A. Demeyer, C. Pastor, A. Giorni, A. Lleres, P. Stassi, J. B. Viano, and P. Gonthier, *Phys. Rev. Lett.* **68**, 2141 (1992).
- [3] G. Bizard, D. Durand, A. Genoux-Lubain, M. Louvel, R. Bougalt, R. Brou, H. Doubre, Y. El-Masri, H. Fugiwara, K. Hagel, A. Hajfani, F. Hanappe, S. Jeong, G. M. Jin, S. Kato, J. L. Laville, C. Le Brun, J. F. Lecolley, S. Lee, T. Matsuse, T. Motobayashi, J. P. Patry, A. Peghaire, J. Peter, N. Prot, R. Regimbart, F. Saint-Laurent, J. C. Stockmeyer, and B. Tamain, *Phys. Lett. B* **276**, 413 (1992).
- [4] J. Boger, S. Kox, G. Auger, J. M. Alexander, A. Narayanan, M. A. McMahan, D. J. Moses, M. Kaplan, and G. P. Gilfoyle, *Phys. Rev. C* **41**, R801 (1990).
- [5] J. Boger and J. M. Alexander (unpublished).
- [6] D. J. Moses, Ph.D. dissertation, Dept. of Chemistry, Carnegie Mellon University (1986).
- [7] J. Boger, Ph.D. dissertation, Department of Chemistry, SUNY Stony Brook (1992).
- [8] J. Boger, J. M. Alexander, G. Auger, A. Elmaani, S. Kox, R. Lacey, A. Narayanan, M. Kaplan, D. J. Moses, M. A. McMahan, P. A. DeYoung, C. J. Gelderloos, and G. Gilfoyle, accompanying paper, *Phys. Rev. C* **49**, 1576 (1994).
- [9] R. J. Charity, D. R. Bowman, Z. H. Liu, R. J. McDonald, M. A. McMahan, G. J. Wozniak, L. G. Moretto, S. Bradley, W. L. Kehoe, and A. C. Mignerey, *Nucl. Phys.* **A476**, 516 (1988).
- [10] R. J. Charity, M. A. McMahan, G. J. Wozniak, R. J. McDonald, L. G. Moretto, D. G. Sarantites, L. G. Sobotka, G. Guarino, A. Pantaleo, L. Fiore, A. Gobbi, and K. D. Hildenbrand, *Nucl. Phys.* **A483**, 371 (1988).
- [11] L. G. Moretto, *Nucl. Phys.* **A247**, 211 (1975).
- [12] C. J. Gelderloos, J. M. Alexander, J. Boger, P. DeYoung, A. Elmaani, M. T. Magda, A. Narayanan, J. Sarafa (unpublished data, 1990).
- [13] V. E. Viola, K. Kwiatkowski, S. J. Yennello, and D. E. Fields, in *Proceedings of the Symposium on Nuclear Dynamics and Nuclear Disassembly*, Dallas, Texas, 1989, edited by J. B. Natowitz (World Scientific Publishers, Singapore, 1989), p. 82.
- [14] R. P. Schmitt and A. J. Pacheco, *Nucl. Phys.* **A379**, 313 (1982).
- [15] D. J. Moses, M. Kaplan, J. M. Alexander, D. Logan, M. Kildir, L. C. Vaz, N. N. Ajitanand, E. Duek, and M. S. Zisman, *Z. Phys. A* **320**, 229 (1985).
- [16] L. G. Moretto and G. J. Wozniak, *Progr. Part. Nucl. Phys.*, **21**, 401 (1988).
- [17] L. C. Vaz, D. Logan, J. M. Alexander, E. Duek, D. Guereau, L. Kowalski, M. F. Rivet, M. S. Zisman, *Z. Phys. A* **311**, 89 (1983).
- [18] W. E. Parker, Ph.D. dissertation, Dept. of Chemistry, Carnegie Mellon University (1989).
- [19] See, for example, M. S. Gordon, R. L. McGrath, G. Auger, J. M. Alexander, D. G. Kovar, M. F. Vineyard, C. Beck, D. J. Henderson, P. A. DeYoung, and D. Kortering, *Phys. Rev. C* **46**, 265 (1992).